Coulomb Asymmetry in Strong Field Multielectron Ionization of Diatomic Molecules

J. Wu,[1,2] M. Meckel,[1] S. Voss,[1] H. Sann,[1] M. Kunitski,[1] L. Ph. H. Schmidt,[1] A. Czasch,[1] H. Kim,[1]
T. Jahnke,[1] and R. Dörner[1,*]

[1]*Institut für Kernphysik, Goethe Universität, Max-von-Laue-Strasse 1, D-60438 Frankfurt, Germany*
[2]*State Key Laboratory of Precision Spectroscopy, East China Normal University, Shanghai 200062, China*

We measure the angular distribution of an electron emitted by a strong elliptically polarized two-color laser field from exploding doubly charged molecular nitrogen. This angular distribution is vastly different for emission of the electron from the up-field core of the molecule as compared to that from the down-field core. The emission from the down-field core leads to a slight rotation with respect to the internuclear axis in the direction expected by the Coulomb effect of the remaining ion, while, for the emission from the up-field core, this direction is inversed. Our semiclassical simulations suggest that this unexpected angular distribution is caused by an initial longitudinal momentum of the electron freed by over-the-barrier ionization above the inner barrier in the molecule. The initial kinetic energy is in the range of the potential energy of the Stark-shifted orbital above the barrier.

What is the influence of the remaining ionic core on an electron wave emitted from an atom or molecule and on the ionization process itself? This question is general across all ionization phenomena. For atomic single-photon ionization, the Coulomb potential gives rise to a phase shift, and the relationship of this phase shift to the time the photoeffect takes is a topic of controversial debate [1]. For molecular single photoionization, in this case, the asymmetric potential shapes the angular distributions and gives rise to shape resonances [2]. For ionization by charged particle impact (electron or ion), the ion potential poses a major challenge in the calculation and modifies energy and angular distributions of the emitted electron [3]. For ionization by a strong laser field, the Coulomb potential of the parent ion on the escaping electron gives rise to many interesting effects, such as the asymmetric above-threshold ionization spectra [4–6], Coulomb focusing [7–9], low-energy photoelectrons in midinfrared wavelengths [10,11], and recapture of Rydberg electrons [12–14].

For strong laser field ionization, the electron tunnels to the continuum through the strong field-suppressed potential barrier. Its succeeding motion is primarily driven by the oscillation of the subsequent laser field [15,16] and influenced by the Coulomb potential when the tunnel exit of the electron is in the vicinity of the parent ion. This influence will become more significant in the case of the multielectron ionization where a multiply charged ionic core is created. However, most of the Coulomb potential studies are focused on atoms so far. In the present Letter, we show that, for a diatomic molecule, the Coulomb effect in strong field ionization has a very different influence on the electron dynamics than the case of atom, strongly depending on from which side of the molecule the electron is set free.

We study the case of sequential multiple ionization of N_2. Following double ionization, the diatomic molecular

ion starts to explode. At some time later, the third electron can be freed by the laser field from one of the dissociating atomic ions, leading to the charge asymmetric exploding channel $N^{2+} + N^+$. We study the final momentum distribution of the freed third electron. By using a phase-controlled elliptically polarized two-color ultrashort laser pulse, we distinguish the electron freed from the up-field (leading to the N^{2+} on the up-field side) or down-field cores (leading to the N^{2+} on the down-field side) of the diatomic molecule [Fig. 1(c)]. We find a strong Coulomb potential effect on the angular distribution of the electron when it is freed from the down-field core, while the electron escapes from the molecular ion rapidly when it is freed from the up-field core and thus experiences a negligible Coulomb potential effect and results in a significantly different angular distribution.

Experimentally, the phase-controlled elliptically polarized two-color pulse is generated in a collinear scheme. For this purpose, a linearly polarized femtosecond laser pulse from a Ti:Sapphire laser system (35-fs, 790 nm, 8 kHz) is first frequency-doubled using type I phase matching in a 200 μm thick β-barium borate (β-BBO) crystal. The time lag between the fundamental-wave (FW) and second-harmonic (SH) pulses is compensated with a birefringent α-BBO crystal by orienting its fast axis along the SH polarization. A dual-wavelength half-wave plate ($\lambda/2$ for FW and λ for SH) is then used to rotate the FW polarization to be parallel to that of the SH. After a quarter-wave plate centered at the SH wavelength (the fast axis is 45° orientated with respect to the input polarization), the linear polarization of the two-color pulse is changed to be elliptical. By tuning the insert thickness of a fused silica wedge pair in the beam line, we can vary the absolute phase $\Delta\Phi$ (or the relative phase between the FW and SH components) of the two-color pulse from 0 to π. This alters the field
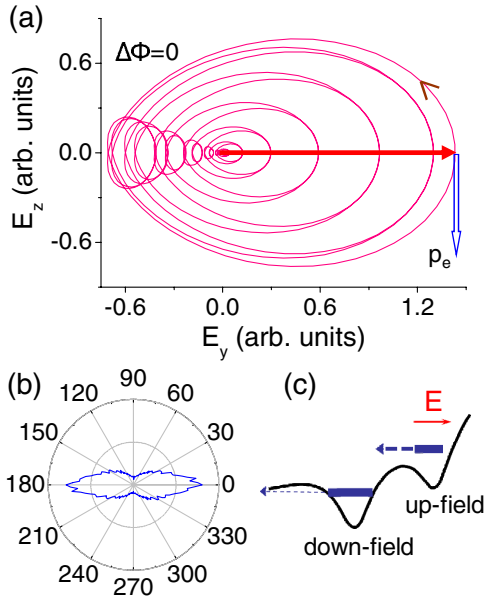
FIG. 1 (color online).   (a) The sketch of the elliptically polarized two-color pulse and the angular streaking concept in our coordinate system. Its major axis is along y and the minor along z. For the absolute phase of $\Delta\Phi = 0$, an electron freed at a certain instantaneous field points to $+y$ (solid red arrow) and receives a final momentum after the pulse points to $-z$ (open blue arrow) in the polarization plane driving solely by the rotating vector of the laser field. (b) The angular distribution of the explored $N^+ + N^+$ channel. (c) The field-dressed double well potential of the diatomic molecular ion.

maximum of the two-color pulse to be pointing in the positive or negative directions of the major axis of the polarization ellipse. The phase-controlled elliptically polarized two-color pulse is then used to ionize diatomic molecule N_2 in the reaction microscope of COLd Target Recoil Ion Momentum Spectroscopy (COLTRIMS) [17,18]. The intensities of the FW and SH pulses are estimated to be 7.6×10^{14} and 3.4×10^{14} W/cm^2, respectively. The momentum vectors of correlated ions and electrons are measured by two time- and position-sensitive detectors [19] on opposite sides of the spectrometer. Nevertheless, as we will show later, for the exploded multielectron ionization channel, the ion momenta carry all the information we need, so the detected electron is used for calibration purposes only.

Figure 1(a) schematically illustrates the elliptically polarized two-color pulse produced in our experiment, whose major axis is along the y axis. By considering the sole driving of the laser field, the freed electron acquires a final momentum approximately perpendicular to the instantaneous field vector at the moment of ionization [15], which is named as the "angular streaking" [20,21]. This momentum will lie along the negative (or positive) direction of the z axis for $\Delta\Phi = 0$ (or π) with the pulse maximum pointing to the positive (or negative) direction of the y axis. In order to calibrate the absolute phase $\Delta\Phi$ of our two-color ellip-

tical pulse, for moderate laser intensity, we coincidently measured the momentum distributions of the singly ionized atomic ion Ar^+ and the ejected electron by scanning the insert thickness of the fused silica wedge pair. By analyzing the momentum asymmetry of the coincident ions and electrons along the z axis, we were able to determine the absolute phase of the elliptically polarized two-color pulse, which is fairly straightforward and robust as compared to that of the linear polarization [22]. However, most importantly, the use of the elliptically polarized laser field for ionization allows us to avoid the unwanted rescattering [20,21] and Coulomb focusing [7–9] processes, which could have a thorough impact on the electron emission dynamics.

The angular distribution of the ionic fragments of the exploded $N^+ + N^+$ channel is shown in Fig. 1(b). In agreement with experiments using linearly polarized light [23], we find that those molecules aligned parallel to the major axis of the field are predominantly multiply ionized. Therefore, for the following analysis, we have selected only ions emitted within a 30° cone with respect to the major polarization axis (y axis).

The measured ion sum-momentum distributions of the exploded $N^+ + N^+$ channel following the double ionization of N_2 are displayed in Figs. 2(a) and 2(b). Because of the momentum conservation, the sum of all electron momentum vectors is the inverse of the sum of all ion momentum vectors. Therefore, Figs. 2(a) and 2(b) indeed depict the sum-momentum distribution of the freed two electrons of the $N^+ + N^+$ channel. The dominated distribution in the positive (or negative) space of the z axis reflects the "angular streaking" [20,21] by our elliptically polarized two-color pulse with $\Delta\Phi = 0$ (or π). The correlated molecular ion receives an equivalent momentum in the opposite direction according to the momentum conservation, whereas its asymmetric distribution along the y axis shows the influence of the Coulomb potential of the molecular ion on the outgoing electron. This asymmetry can be clearly seen in Fig. 2(e) by plotting it as the angular distribution. For the elliptical two-color pulse of $\Delta\Phi = 0$, the electron tunnels to the continuum at the negative side of the y axis ($-y$), since it is mostly freed when the laser field points to $+y$. This electron will experience an attractive Coulomb force of its parent ion in the direction of $+y$, acquiring additional momentum along $+y$. Correspondingly, the resulting ion sum-momentum distribution (i.e., joint electron recoil) of the exploded doubly charged molecule shifts to $-y$. Likewise, this Coulomb potential effect shifts the ion sum momentum to $+y$ when the absolute phase of the two-color pulse is switched to $\Delta\Phi = \pi$.

The most interesting information about the Coulomb effect can be obtained for the third electron which escapes from the $N^+ + N^+$. As shown in Fig. 1(c), this electron can either be born on the down-field side or from the up-field
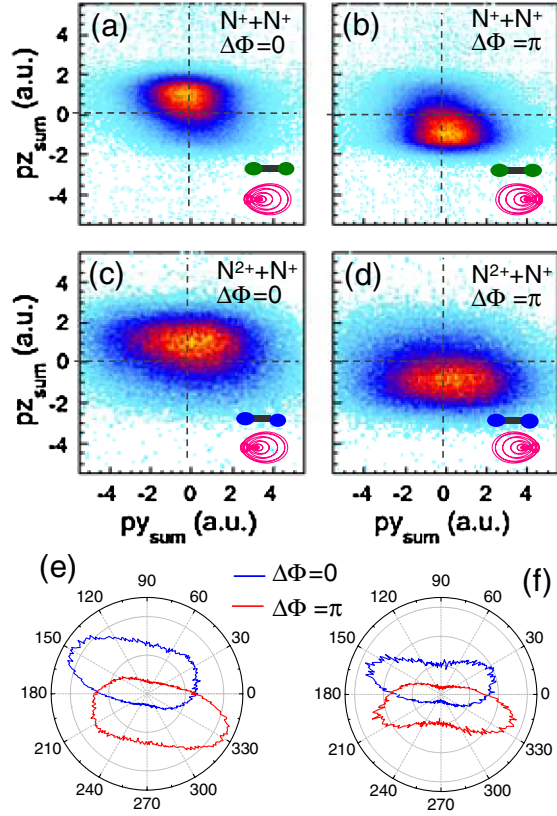
FIG. 2 (color online).   (a)–(d) The ion sum-momentum distributions of the exploded doubly ($N^+ + N^+$) and triply ($N^{2+} + N^+$) ionized N_2. The corresponding angular distributions are plotted in (e) $N^+ + N^+$ and (f) $N^{2+} + N^+$. The intensities of the FW and SH pulses are estimated to be 7.6×10^{14} and 3.4×10^{14} W/cm^2, respectively. The elliptical two-color laser field and the orientation of the molecule are shown as the insets.
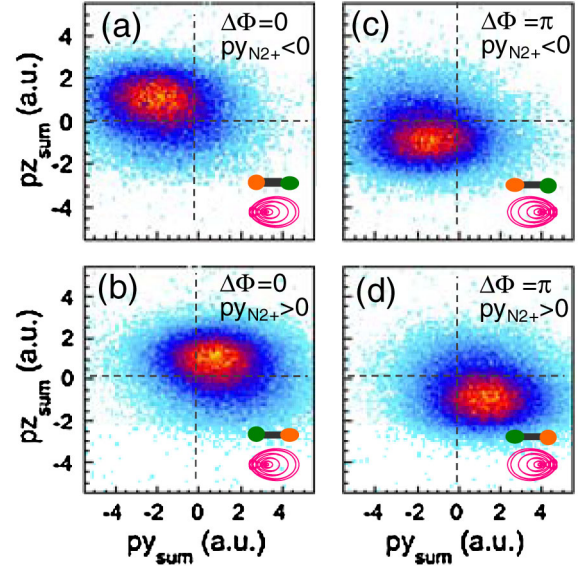

FIG. 3 (color online).   The ion sum-momentum distributions of the $N^{2+} + N^+$ channel when the emission direction of the doubly charged ion N^{2+} is gated. For $\Delta\Phi = 0$ (or π), the third electron is freed from the (a) down-field [or (c) up-field] or (b) up-field [or (d) down-field] core of the diatomic molecular ion when the doubly charged ion N^{2+} emits to $-y$ ($py_{N2+} < 0$) or $+y$ ($py_{N2+} > 0$), respectively. The insets show the elliptical two-color laser field and the orientation of the molecule.

side, which will experience different molecular potentials and thus different dynamics. The measured ion sum-momentum distributions of the exploded $N^{2+} + N^+$ channel are displayed in Figs. 2(c) and 2(d). The corresponding angular distributions are plotted in Fig. 2(f). It reflects the sum-momentum distribution of the freed three electrons. Similar to the $N^+ + N^+$ channel, the ion sum momentum of the $N^{2+} + N^+$ channel dominates in the $+z$ (or $-z$) space and slightly shifts to the $-y$ ($+y$) direction when $\Delta\Phi = 0$ (or π). It is due to the combining result of the angular streaking of the rotating laser field and the attraction of the Coulomb potential of the molecular ion.

For the charge asymmetric exploding channel of $N^{2+} + N^+$, the phase-controlled elliptically polarized two-color pulse allows us to distinguish that the third electron is freed from the up-field or down-field cores of the molecule. Namely, for $\Delta\Phi = 0$, Figs. 3(a) and 3(b) illustrate the ion sum-momentum distributions of $N^{2+} + N^+$ for the cases in which the doubly charged ion N^{2+} emits to the $-y$ ($py_{N2+} < 0$) or $+y$ ($py_{N2+} > 0$) directions, which correspond to when the third electron is freed from the down-field or up-field cores of the molecular ion,

respectively. In the elliptically polarized pulse, the rescattering process is mostly suppressed, and the multielectron ionization proceeds mainly through sequential steps [20]. We therefore can extract the momentum of the third electron (inverse of the recoiled momentum of the molecular ion) from the ion sum momentum of the $N^{2+} + N^+$ channel by performing two-dimensional deconvolution of it with that of the $N^+ + N^+$ channel. The result of this deconvolution is shown in Figs. 4(a) and 4(b). The deconvolution procedure assumes that the third ionization step is independent from the first two, and hence the sum momentum for triple ionization is the convolution of the momentum for double ionization with the momentum of the third step. The third electron freed from the down-field core ($py_{N2+} < 0$) behaves as expected: the electron mostly tunnels to the continuum with an initial exit at $-y$ in the vicinity of the parent ion when the field vector points to $+y$; the rotating laser field streaks its momentum by 90° to $-z$; meanwhile, the attraction of the Coulomb potential of the parent core shifts its momentum to $+y$ and results in the dominated electron momentum distribution in the fourth quadrant [Fig. 4(a)]. However, the third electron freed from the up-field core ($py_{N2+} > 0$) shows a surprising momentum distribution in the third quadrant [Fig. 4(b)], opposite to the exception of the Coulomb potential effect of the parent ion. The corresponding angular distributions are plotted in Fig. 4(e). This interesting difference in the momentum distributions of the third
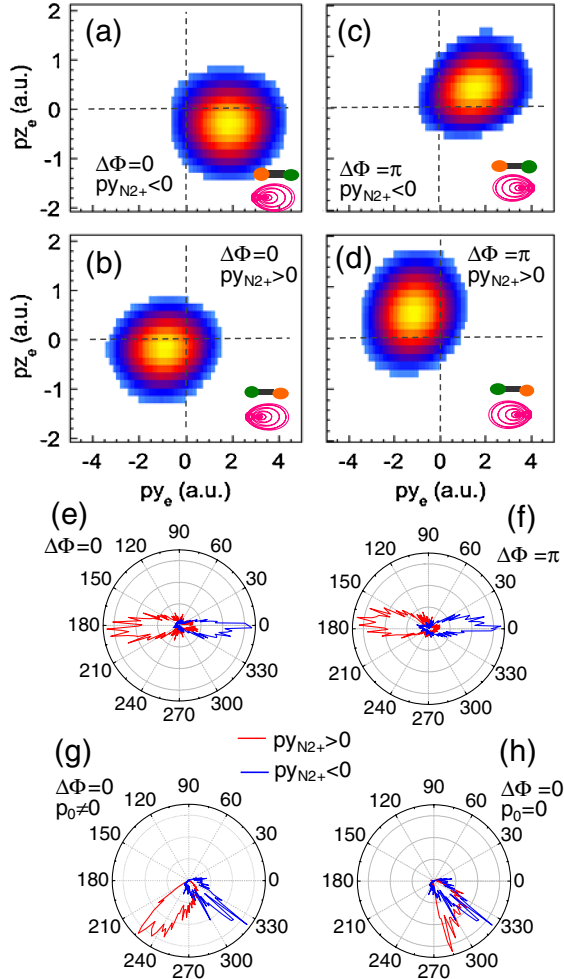
FIG. 4 (color online).   (a)–(d) The deconvoluted momentum of the third electron freed from different sides of the molecules for the $N^{2+} + N^+$ channel. The corresponding angular distributions are plotted in (e),(f). (g),(h) The simulated angular distributions of the third electron freed from $N^{2+} + N^+$ by a two-color elliptical pulse of $\Delta\Phi = 0$, where an initial longitudinal momentum is (g) considered or (h) switched off, respectively. The insets show the elliptical two-color laser field and the orientation of the molecule.

electron when it is freed from the up-field or down-field cores is well-reproduced when the absolute phase of the two-color elliptical pulse is switched to $\Delta\Phi = \pi$ [see Figs. 3(c), 3(d), 4(c), 4(d), and 4(f)], ruling out the systematic error of the measurement and analysis.

To understand the observed angular distributions of the third electron when it is freed from different sides of the diatomic molecular ion, we performed a semiclassical simulation by considering an initial tunneling ionization step and then a subsequent classical propagation of the freed electron driven by the succeeding laser field and the Coulomb potential of the molecular ion. The diatomic molecular ion consists of singly and doubly charged atomic ions localized along the y axis. The third electron is

assumed to be freed from the doubly charged atomic ion with an ADK (Ammosov-Delone-Krainov) ionization rate [24]. For the third electron freed at time t_0, the ionization potential is set to be $I_p(t_0) = 2I_{p0} + 1/R - E_y(t_0)R/2$ [25], where I_{p0} is the single ionization potential of a neutral nitrogen atom and $E_y(t_0)$ is the time-dependent laser electric field along the molecular axis. The third term $E_y(t_0)R/2$ stands for the Stark shift of the electron energy by the laser field [25–27]. For the electron tunnels through the field-dressed barrier at moderate laser intensity, the exit is determined by the equation of $U(x, y) + (xE_x + yE_y) = -I_p$, where $U(x, y)$ is the field-free potential of the diatomic molecular ion [25–27]. For the over-barrier ionization at high laser intensity, the tunnel exit of the electron is put at the saddle point of the field-dressed potential, and an initial longitudinal momentum in the direction opposite to the instantaneous laser field vector is applied to accommodate for the energy difference between the ionization potential and the saddle point [21].

Taking the two-color elliptical pulse with an absolute phase of $\Delta\Phi = 0$ as an example, Fig. 4(g) plots the simulated angular distributions of the third electron when it is freed from the up-field or down-field cores, respectively, which qualitatively agree with our experimental measurements. For the diatomic molecular ion, the ionization potential of the electron at the down-field core is increased due to the Stark effect [25–27] of the applied laser field. This electron is freed mostly by tunneling through the broad outer barrier to the continuum when the laser field vector points to $+y$, which experiences a regular Coulomb attraction of the molecular ion and receives a final momentum in the fourth quadrant, whereas the Stark effect raises the energy of the electron at the up-field core [25–27], increasing the over-barrier ionization probability. This electron, with a considerable initial longitudinal momentum in the direction opposite to the instantaneous laser field vector, escapes from the molecular ion rapidly and sees negligible Coulomb potential of the parent ion. Its final momentum is thus determined by the initial momentum and the streaking of the subsequent laser field. Since this electron is most pronouncedly freed when the laser field points to $+y$ for the two-color elliptical pulse of $\Delta\Phi = 0$, it ends with momentum angular distribution in the third quadrant [Fig. 4(g)]. When the initial longitudinal momentum is switched off, as plotted in Fig. 4(h), the electron freed from the up-field core also experiences a strong Coulomb attraction of the molecular ion and shows an angular distribution in the fourth quadrant similar to that freed from the down-field core. Very recently, this effect of the initial longitudinal momentum of the tunneling electron on its final momentum distribution was also observed in the single ionization of the molecular ion H_2^+ by using a circularly polarized ultrashort laser pulse [28]. Interestingly, the initial longitudinal momentum of the first tunneling electron was found to be important for

understanding the entire nonsequential double-ionization process [29].

In summary, by using a phase-controlled elliptically polarized two-color ultrashort laser pulse, we experimentally observed significant different angular distributions of the third electron when it is freed from the up-field or down-field cores of an exploding doubly charged diatomic molecular ion. The semiclassical simulation qualitatively agrees with the experimental observations, indicating that the initial longitudinal momentum contributes to the unexpected momentum distribution of the electron freed from the up-field core, whereas the final momentum of the electron freed from the down-field core is mainly determined by the Coulomb attraction of the parent ion. Our results demonstrate the strong Coulomb asymmetry in the multielectron ionization of diatomic molecules and will shed some light on the understanding and controlling of the rich behavior of molecules in strong laser fields.

---

*doerner@atom.uni-frankfurt.de

[1] M. Schultze *et al.*, Science **328**, 1658 (2010).
[2] M. Piancastelli, J. Electron Spectrosc. Relat. Phenom. **100**, 167 (1999).
[3] M. Unverzagt *et al.*, Phys. Rev. Lett. **76**, 1043 (1996).
[4] M. Bashkansky, P. H. Bucksbaum, and D. W. Schumacher, Phys. Rev. Lett. **60**, 2458 (1988).
[5] G. G. Paulus *et al.*, Phys. Rev. Lett. **84**, 3791 (2000).
[6] S. P. Goreslavski *et al.*, Phys. Rev. Lett. **93**, 233002 (2004).
[7] T. Brabec, M. Yu. Ivanov, and P. B. Corkum, Phys. Rev. A **54**, R2551 (1996).
[8] D. Comtois *et al.*, J. Phys. B **38**, 1923 (2005).
[9] C. Huang, Q. Liao, Y. Zhou, and P. Lu, Opt. Express **18**, 14 293 (2010).
[10] C. I. Blaga *et al.*, Nature Phys. **5**, 335 (2009).
[11] W. Quan *et al.*, Phys. Rev. Lett. **103**, 093001 (2009).
[12] T. Nubbemeyer *et al.*, Phys. Rev. Lett. **101**, 233001 (2008).
[13] U. Eichmann *et al.*, Nature (London) **461**, 1261 (2009).
[14] J. Wu *et al.*, Phys. Rev. Lett. **107**, 043003 (2011).
[15] P. B. Corkum, N. H. Burnett, and F. Brunel, Phys. Rev. Lett. **62**, 1259 (1989).
[16] P. B. Corkum, Phys. Rev. Lett. **71**, 1994 (1993).
[17] J. Ullrich *et al.*, J. Phys. B **30**, 2917 (1997).
[18] R. Dörner *et al.*, Phys. Rep. **330**, 95 (2000).
[19] O. Jagutzki *et al.*, Nucl. Instrum. Methods Phys. Res., Sect. A **477**, 244 (2002).
[20] P. Eckle *et al.*, Nature Phys. **4**, 565 (2008).
[21] A. N. Pfeiffer *et al.*, Nature Phys. **8**, 76 (2012).
[22] D. Ray *et al.*, Phys. Rev. A **83**, 013410 (2011).
[23] A. S. Alnaser *et al.*, Phys. Rev. Lett. **93**, 113003 (2004).
[24] M. V. Ammosov, N. B. Delone, and V. P. Krainov, Zh. Eksp. Teor. Fiz. **91**, 2008 (1986) [Sov. Phys. JETP **64**, 1191 (1986)].
[25] S. Chelkowski and A. D. Bandrauk, J. Phys. B **28**, L723 (1995).
[26] T. Seideman, M. Yu. Ivanov, and P. B. Corkum, Phys. Rev. Lett. **75**, 2819 (1995).
[27] T. Zuo and A. D. Bandrauk, Phys. Rev. A **52**, R2511 (1995).
[28] M. Odenweller *et al.*, Phys. Rev. Lett. **107**, 143004 (2011).
[29] X. L. Hao, W. D. Li, J. Liu, and J. Chen, Phys. Rev. A **83**, 053422 (2011).